CHAPTER-1

Introduction and Review

If molecular electronics will finally prove to be viable technologies, it is quite clear that quantum physics will change from basic to applied science, and physicists will work and be regarded as electrical engineers...

1.1 Molecular Electronics: An Introduction

1.1.1 Origin

Since the introduction of the integrated circuit in the late 1950s, the number of individual transistors that can be placed upon a single integrated circuit chip has approximately quadrupled every three years (Moore's law- the number of transistors on a single integrated circuit chip roughly doubles every 18 months). The fact that more functionality can be put on a chip when there are more transistors, coupled to the fact that the basic cost of the chip (in terms of $\$/cm^2$) has changed very little from one generation to the next (until recently), leads to the conclusion that greater integration leads to a reduction in the basic cost per function for high-level computation as more functions are placed on the chip. It is this simple functionality argument that has driven device feature reduction according to a complicated scaling relationship. In 1980, Hewlett-Packard produced a single-chip microprocessor containing approximately half million devices in its 1 cm^2 area. This chip was produced with transistors having a nominal 1.25 mm gate length and was considered a remarkable step forward. In contrast, by 2007, the printed gate length of production microprocessor transistors was 48 nm and the physical gate length was closer to 25 nm. Research devices have been demonstrated down to 10 nm gate length or less. Clearly, current integrated circuit manufacturing is truly a nanoscale technology. For a 25 nm gate length Si device, the number of atoms spanning the channel is on the order of a 100 or less. It has been concluded that one can easily downsize the transistor to a gate length of 30 nm if macroscopic transport theory

continued to hold. There were predictions [www.itrs.net] of scaling down to 10 nm gate length before a serious "brick wall" is encountered and 15 nm gate lengths are scheduled for production by 2010. Laboratory MOSFET devices with gate lengths down to 15 nm have been reported by Intel [1] and AMD [2] which exhibit excellent I–V characteristics, and 6 nm gate length p-channel transistors have been reported by IBM [3].

The (slow) death of Moore's law has been the main driver of progress in today's information and communications society. One of the possible routes by which the current technology can be improved, is called "Beyond Moore" and it includes radically new system architectures whose building blocks may be atomic and molecular devices, and also the substitution of Boolean logic by more efficient algorithms, possibly based on quantum computation. Very clever designs are pushing the limits of today's CMOS technology even further, since as Gordon Moore put it, "No Exponential is forever, but we can delay 'forever' ". But there is no doubt that in the end the venerable CMOS micro- and even "nano-electronics" technology must give way to radically new approaches, that will be based in quantum physics and chemistry, like graphene electronics, or molecular electronics [4, 5] or spinotronics.

As in every business matter, the demise of a long-standing main actor in the play, and the rise of new stars must be viewed not as a catastrophic event, but rather as the scenario where a new wealth of opportunities arises. For instance, organic molecules with tailored shapes and functionalities can be made and assembled with the various techniques like such as the scanning tunneling microscope (STM), transmission electron microscope (TEM), mechanically controllable break junctions, atomic force microscopy (AFM), and high resolution transmission electron microscopy (HRTEM) to realize molecular circuits [6-14]. This fascinating and extremely powerful approach is expected to decrease the minimum feature size of electronic devices even below the 1 nm mark, giving rise to an increase of orders of magnitude in the number of devices that can be packed in a chip. The same

quantum tunnelling effect that produces heating in today's computers can be used to produce the main signal in a molecular FET, thereby reducing heating effects. Extremely fast memories can be fabricated by the use of molecules where precise control of the switching between two molecular states can be achieved by external means. Boolean logic gates can be fabricated that do not use the FET concept. Furthermore, precise control of the electronic states in a molecule should allow the replacement of Boolean by quantum logic, where extremely more powerful algorithms should lead to an exponential increase in the processing power of computers. The performance of the all-important contacts between a logic device and the circuitry in the chip will ultimately be controlled to unimaginable levels by suitable chemical bond engineering. The low performance of semiconductor optoelectronics will be possibly overhauled by dedicated circuits. In which, optically active molecules would be tailored to either receive or emit the electromagnetic radiation of given wavelengths.

1.1.2 Exotic effects and potential

Even though molecular electronics is a relatively new field the advances in this area of research have been significant. Molecules have a series of advantages over the traditional silicon based lithographic techniques. Besides the obvious huge increase in packing density of electronic components, they can be synthesized easily and with low cost in many cases; they can be grown in three dimensions as opposed to the typical 2D semiconductor lithographic layout; they can self-assemble; they are expected to reduce heat and noise production and, most importantly, they can display a whole new world of properties and functionalities.

Recent growing interest in making electronic devices using molecules comprising of Carbon chains or benzene rings aims at replacing standard semiconductors with organic materials.

They have the advantages of being produced with low-temperature low-cost chemical methods, instead of expensive high-temperature solid-state growth (e.g. molecular beam epitaxy) and patterning (lithography) techniques. In addition the endless possibilities of chemical synthesis, end-group and side-chain engineering give good expectation for new concept devices. From the electronic side negative differential resistance [15] and rectification [16] have already been proved at the molecular level and fully functional molecular transistors [17], memories and logic gates [18, 19] have been demonstrated suggesting a possible road-map to the post-silicon era. They should produce future generations of computers, together with magnetic data storage devices exceeding the Terabit/in^2 storage limit. The readout of such high-density data storage media will be achieved using nanoscale devices with magnetic atomic point contacts [20, 21]. Since the seminal work of Reed et al. [10], several experiments have been performed on a variety of molecules [6, 15-17, 22-26]. Although the feasibility of single molecule devices has been shown, a number of issues have been raised by these experiments. Probably the most important of them is the nature of the contact between the molecule and the surface of the electrodes. One of the fundamental aspects of molecular electronics is that the bonding between a molecule and the current/voltage probes can dramatically change the current flowing through a device compare to conventional inorganic heterostructures. The bonding site and the bond angle usually depend on the layer density (coverage), and these can be further tuned by changing the anchoring groups. Ultimately we can say that molecules present great potential but also introduce new complications, especially from the fabrication point of view. Greater control and characterisation is necessary when designing devices.

1.1.3 Computing electronic transport

Alongside of large experimental investigations and explorations on nanoscale devices, equally large efforts have been devoted to develop efficient computational methods for evaluating conduction characteristics of nanoscale devices. Simullteneously or many times way ahead of experimental progress, there have been theoretical/ computational works predicting and analysing the physics behind the transport of electrons through molecular junctions. This is a great theoretical challenge since advanced quantum transport algorithms must be combined with state of the art electronic structure methods. Modern theory of quantum transport has developed a range of methods for calculating transport in nanoscale conductors.

Various methods which are used for computing study of electronic transport can be divided in following categories:

1. Methods based on Landauer-type scattering formalism in combination with ground state DFT [27-35]. They are based upon the assumption that, regardless of the details of a possible transient, a steady state is always achieved. These methods are widely used for ballistic as well as non equilibrium conductance calculations.
2. Another three alternate approaches are,
    a. Use of Kohn–Sham effective single-particle version of a 'master equation' formulation of transport [36-38].
    b. With the use of time dependent DFT (TDDFT), one obtains the current by calculating the time evolution of a system consisting of a molecule coupled to two finite metallic contacts and turning on a potential step, resulting in two different chemical potentials [39].
    c. A method that uses large finite leads, and watches a capacitance discharge [40].

Methods described above essentially begin from a static distribution, apply some change, and allow the system to evolve to a steady, but non-equilibrium distribution. For non-interacting electrons in the weak bias limit, all agree, both with each other and the standard approach, but likely disagree in the general case of interacting electrons in finite bias. Under certain limiting conditions, such as adiabatic approximations to TDDFT, and local approximations to ground-state DFT, they yield the same results.

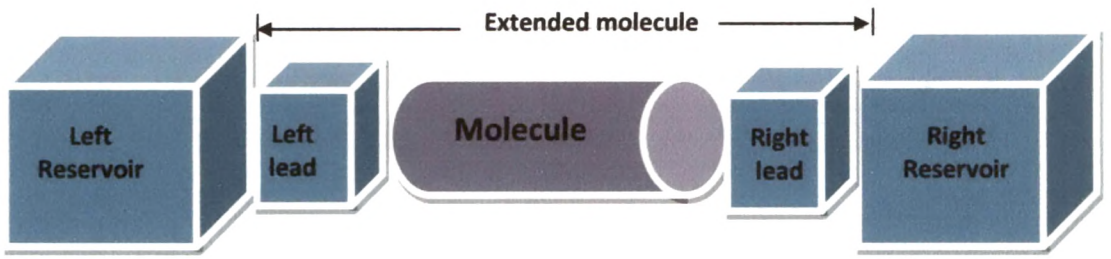

Figure 1.1.1: Schematic diagram used for electronic transport calculation of nanostructures.

A schematic drawing of a molecular junction is shown in Fig. 1.1, where one or more molecules are sandwiched between two semi-infinite electrodes. Mainly, the junction used in molecular electronics has three parts:

(1) The electrodes or reservoirs,

(2) The backbone of the molecule, and

(3) The interfaces between lead and the molecule.

These three parts contribute to the total transmission of electrons through the junction. Changing any physical or chemical aspect of any part is manifested in drastic change in behaviour of electron transport through the junction. There have been large number of first

principle investigations on various aspects of a molecular devices such as the material-dependent effects, structures and relaxation of electrodes [41-44], effect of electrode work function [45], Fermi level alignment [46, 47], interface/ contact dependence [48], effects of roughness of interface [49, 50], tilt-angle and temperature-dependence [51], effects of functional, anchoring and side groups [52, 53], importance of geometry over chemistry [54], effects of molecular symmetry [55], molecular conformation [56] and molecular length dependence [57-61].

The conductance properties of atomic chains of different length [62, 63, 64], atomic clusters of different sizes [65, 66], cage structures having different number and types of impurities [67], graphene sheets [68, 69], passivated and non-passivated nanoribbons [70, 71, 72] of different width and length, SW, DW and MW nanotubes [73, 74] of different diameter and chirality, nanotubes with impurities and defects [75], benzene [76.77], molecules made by number of phenyl rings [78] and having different groups attached on different sites of it [79], polyynes [80, 81], alkane and alkenes [82, 83, 84, 85] are very well studied, exploring new phenomenon and searching for science behind them and giving answers to many queries. There still remain many unanswered questions and there are also newly aroused questions from recent discoveries that should be addressed properly.

For a very small or no external bias voltage applied to the electrodes, one can assume the electrode-scatterer-electrode system in equilibrium. This linear regime is useful to study the adsorption induced modifications in electronic structure of electrode-molecule-electrode system which are more dominant than field induced modification. Due to nanometric size of molecules used as the scatterer in nanodevices, the length of the scatterer is essentially smaller than the mean free path of the electron. Therefore, the electrons incident on one electrode-molecule junction can be considered to reach at the other junction without

experiencing any scattering within the scatterer. This type of electron transport is known as ballistic transport.

Mainly, Carbon based molecular devices, which have aromatic rings or alkanes and structures like fullerene, nanotubes, graphene, nanoribbon and graphane are widely considered, as they are characterized by an amazingly large variety of structures and the properties that originate from the combination of *sp*, sp^2 and sp^3 hybridisations of Carbon atoms. The main parameters that affect the transport properties of two probe molecular devices are related to:

(i) Change in geometry/chemistry of molecules.

(ii) Change in geometry of contact between molecule and electrode.

(iii) Change in chemistry/geometry/dimensions of electrodes.

The theoretical investigations which are reported in this thesis cover the above mentioned entire aspects in a detailed manner. Meaningful conclusions are drawn from our investigations. Effects of changes in molecular chemistry have been studied by replacing C by isovalent Si atoms in monatomic chains are reported in chapter 2 and effects of change in molecular geometry keeping chemistry of molecules intact have been investigated by taking zigzag (ZZ), armchair (AC) and mixed (COMBO) geometries of molecules made from 2S, 4H and 6C atoms are reported in chapter 3. Effects of change in contact geometry (contact angle) on transport properties have been studied by rotated molecule geometries as reported in chapter 3. Effects of change in edge structure of electrodes (graphene) have been studied and reported in chapter 4. The limitations imposed by the use of Al-nanorod as electrodes on transport through atomic chains have been investigated by taking bulk Al-electrode, in place of nanorod, which is reported in chapter 2. Comparison of transport properties of C atomic chains attached to Al-electrodes and graphene electrodes is also made in chapter 4.

1.2 Basics of DFT and Methodology

1.2.1 Introduction

In quantum mechanics we learn that all information we can possibly have about a given system is contained in the system's wave function. Prediction of the electronic and geometric structure of atoms, molecules and solids requires calculation of the quantum- mechanical total energy and subsequent minimization of that energy with respect to the electronic and nuclear coordinates. Because of the large difference in mass between the electrons and nuclei and the fact that the forces on the particles are the same, the electrons respond essentially instantaneously to the motion of the nuclei. Thus the nuclei can be treated adiabatically, leading to a separation of electronic and nuclear coordinates in the many-body wave function- the so-called Born- Oppenheimer approximation. This reduces the many-body problem to the solution of the dynamics of the electrons in some frozen-in configuration of the nuclei.

Even with the introduction of Born-Oppenheimer approximation, the many-body problem remains formidable. Further simplifications, however, can be introduced that allow total-energy calculations to be performed accurately and efficiently. These include density functional theory (DFT) to model the electron-electron interactions, pseudopotential theory to model the electron-ion interactions, supercells to model systems with aperiodic geometries and iterative minimization techniques to relax the electronic coordinates. Much of what we know about the electrical, magnetic, and structural properties of materials has been calculated using DFT, and the extent to which DFT has contributed to the science of molecules is reflected by the 1998 Nobel Prize in Chemistry, which was awarded to Walter Kohn [86], the founding father of DFT, and John Pople [87], who was instrumental in implementing DFT in

computational chemistry. This approach of DFT forms the basis of the large majority of electronic-structure calculations in physics and chemistry [88-98].

For system with more than one electron (i.e., a many-body problem) Schrodinger's equation becomes

$$\left[\sum_i^N \left(-\frac{\hbar^2 \nabla_i^2}{2m} + v(\mathbf{r}_i)\right) + \sum_{i<j} U(\mathbf{r}_i, \mathbf{r}_j)\right] \Psi(\mathbf{r}_1, \mathbf{r}_2 \ldots, \mathbf{r}_N) = E\Psi(\mathbf{r}_1, \mathbf{r}_2 \ldots, \mathbf{r}_N) \qquad (1.2.1)$$

Where N is the number of electrons and $U(\mathbf{r}_i, \mathbf{r}_j)$ is the electron-electron interaction. For a Coulomb system one has

$$\hat{U} = \sum_{i<j} U(\mathbf{r}_i, \mathbf{r}_j) = \sum_{i<j} \frac{q^2}{|\mathbf{r}_i - \mathbf{r}_j|} \qquad (1.2.2)$$

Note that this is the same operator for any system of particles interacting via the Coulomb interaction, just as the kinetic energy operator

$$\hat{T} = -\frac{\hbar^2}{2m} \sum_i \nabla_i^2 \qquad (1.2.3)$$

is the same for any nonrelativistic system. Whether our system is an atom, a molecule, or a solid thus depends only on the potential $v(\mathbf{r}_i)$. For a molecule or solid e.g.,

$$\hat{V} = \sum_i v(\mathbf{r}_i) = \sum_{ik} \frac{Q_k q}{|\mathbf{r}_i - \mathbf{R}_k|} \qquad (1.2.4)$$

Where the sum on k extends over all nuclei in the system, each with charge $Q_k = Z_k e$ and position $\mathbf{R}_k$. It is only the spatial arrangement of the $\mathbf{R}_k$ (together with the corresponding boundary conditions) that distinguishes, fundamentally, a molecule from a solid. Similarly, it is only through the term U that the (essentially simple) single-body quantum mechanics of differs from the extremely complex many-body problem. These properties are built into DFT in a very fundamental way.

The usual quantum-mechanical approach to Schrodinger's equation (SE) can be summarized by the following sequence

$$v(\mathbf{r}) \xrightarrow{\text{SE}} \Psi(\mathbf{r}_1, \mathbf{r}_2 \ldots, \mathbf{r}_N) \xrightarrow{\langle\Psi|\ldots|\Psi\rangle} \text{observables} \tag{1.2.5}$$

i.e., one specifies the system by choosing $v(\mathbf{r})$, plugs it into Schrodinger's equation, solves that equation for the wave functionΨ, and then calculates observables by taking expectation values of operators with this wave function. One among the observables that are calculated in this way is the particle density

$$n(\mathbf{r}) = N \int d^3r_2 \int d^3r_3 \ldots \int d^3r_N \, \Psi^*(\mathbf{r}_1, \mathbf{r}_2 \ldots, \mathbf{r}_N)\Psi(\mathbf{r}_1, \mathbf{r}_2 \ldots, \mathbf{r}_N) \tag{1.2.6}$$

DFT explicitly recognizes that nonrelativistic Coulomb systems differ only by their potential$v(\mathbf{r})$, and supplies a prescription for dealing with the universal operators $\hat{T}$ and $\hat{U}$once and for all. Furthermore, DFT provides a way to systematically map the many body problem, with$\hat{U}$, onto a single-body problem, without$\hat{U}$. All this is done by promoting the particle density $n(\mathbf{r})$ from just one among many observables to the status of key variable, on which the calculation of all other observables can be based.

The density-functional approach can be summarized by the sequence

$$n(\mathbf{r}) \Longrightarrow \Psi(\mathbf{r}_1, \mathbf{r}_2 \ldots, \mathbf{r}_N) \Longrightarrow v(\mathbf{r}) \tag{1.2.7}$$

i.e., knowledge of $n(\mathbf{r})$ implies knowledge of the wave function and the potential, and hence of all other observables.

1.2.2 The Hohenberg-Kohn-Sham theorem

1.2.2.1 The Hohenberg-Kohn (HK) theorem

The Hohenberg-Kohn (HK) theorem [88, 89] states that for ground states Eq. (1.2.6) can be inverted: given a *ground state* density $n_0(\mathbf{r})$ it is possible, in principle, to calculate the

corresponding *ground-state* wave function$\Psi_0(\mathbf{r}_1, \mathbf{r}_2 \ldots, \mathbf{r}_N)$. This means that Ψ_0 is a functional ofn_0. Consequently, all ground-state observables are functional ofn_0, too.

(a) The nondegenerate ground-state (GS) wave function is a unique functional of the GS density:

$$\Psi_0(\mathbf{r}_1, \mathbf{r}_2 \ldots, \mathbf{r}_N) = \Psi[n_0(r)] \tag{1.2.8}$$

This is the essence of the HK theorem. As a consequence, the GS expectation value of any observable $\hat{O}$ is a functional of$n_0(\mathbf{r})$, too:

$$O_0 = O[n_0] = \langle \Psi[n_0] | \hat{O} | \Psi[n_0] \rangle \tag{1.2.9}$$

The GS energy is one of the most important observable. This energy

$$E_0 = E[n_0] = \langle \Psi[n_0] | \hat{H} | \Psi[n_0] \rangle \tag{1.2.10}$$

Thus, The ground-state energy of a many-body system is a unique functional of the particle density, E_0=E[n(r)]

(b) The functional E[n(r)] has its minimum relative to variations $\delta n(r)$ of the particle density at the equilibrium density $n_0(r)$

$E = E\,[n_0(r)] = \min\,\{E\,[n(r)]\}$

$$\left.\frac{\delta E[n(r)]}{\delta n(r)}\right|_{n(r)=n_0(r)} = 0 \tag{1.2.11}$$

DFT allows one, in principle, to map exactly the problem of a strongly interacting electron gas (in the presence of nuclei) onto that of a single particle moving in an effective nonlocal potential. Although this potential is not known precisely, local approximations to it work remarkably well. At present, we have no arguments to explain why these approximations work however theorists performed total-energy calculations using these potentials and

showed that they reproduced a variety of ground-state properties within a few percent of experiment. Thus, the acceptance of local approximations to DFT has only emerged, a posteriori, after many successful investigations of many types of materials and systems.

1.2.2.2 The Kohn-Sham energy functional

The Kohn-Sham total energy functional for a set of doubly occupied electronic states $\psi_i$can be written as

$$E[\{\psi_i\}] = 2\sum_i \int \psi_i \left[-\frac{\hbar^2}{2m}\right] \nabla^2 \psi_i d^3\boldsymbol{r} + \int V_{ion}(\boldsymbol{r}) n(\boldsymbol{r})\, d^3\boldsymbol{r} + \frac{e^2}{2}\int \frac{n(\boldsymbol{r}) n(\boldsymbol{r}')}{|\boldsymbol{r}-\boldsymbol{r}'|} d^3\boldsymbol{r} d^3\boldsymbol{r}' + E_{xc}[n(\boldsymbol{r})] + E_{ion}(\{\boldsymbol{R}_I\}) \tag{1.2.12}$$

Where E_{ion} is the Coulomb energy associated with interactions among the nuclei (or ions) at positions$\{\boldsymbol{R}_I\}$, V_{ion} is the static total electron-ion potential, $n(\boldsymbol{r})$ is the electronic density given by

$$n(\boldsymbol{r}) = 2\sum_i |\psi_i(\boldsymbol{r})|^2 \tag{1.2.13}$$

And $E_{xc}[n(\boldsymbol{r})]$is the exchange-correlation functional. Only the minimum value of the Kohn-Sham energy functional has physical meaning. At the minimum, the Kohn-Sham energy functional is equal to the ground state energy of the system of electrons with the ions in positions$\{\boldsymbol{R}_I\}$.

1.2.2.3 Kohn-Sham equations

The minimum value of the total-energy functional is the ground-state energy of the system, and the density that yields this minimum value is the exact single-particle ground state

density. Kohn and Sham then showed how it is possible, formally, to replace the many-electron problem by an exactly equivalent set of self-consistent one-electron equations.

It is necessary to determine the set of wave functions that minimize the Kohn-Sham energy functional. These are given by the self-consistent solutions to the Kohn-Sham equations [89]:

$$\left\{\left[-\frac{\hbar^2}{2m}\right]\nabla^2 + V_{ion}(\boldsymbol{r}) + V_H(\boldsymbol{r}) + V_{XC}(\boldsymbol{r})\right\}\psi_i(\boldsymbol{r}) = \varepsilon_i\psi_i(\boldsymbol{r}) \qquad (1.2.14)$$

Where ψ_i is the wave function of electronic state i, ε_i is the Kohn-Sham eigenvalue, and V_H is the Hartree potential of the electrons given by

$$V_H(\boldsymbol{r}) = e^2\int\frac{n(\boldsymbol{r}')}{|\boldsymbol{r}-\boldsymbol{r}'|}\boldsymbol{d}^3\boldsymbol{r}' \qquad (1.2.15)$$

The exchange-correlation potential, V_{XC}, is given formally by the functional derivative

$$V_{XC}(\boldsymbol{r}) = \frac{\delta E_{xc}[n(\boldsymbol{r})]}{\delta n(\boldsymbol{r})} \qquad (1.2.16)$$

The Kohn-Sham equations represent a mapping of the interacting many-electron system onto a system of non- interacting electrons moving in an effective potential due to all the other electrons. If the exchange-correlation energy functional were known exactly, then taking the functional derivative with respect to the density would produce an exchange-correlation potential that included the effect of exchange and correlation exactly.

The Kohn-Sham equations must be solved self-consistently so that the occupied electronic states generate a charge density that produces the electronic potential that was used to construct the equations. Thus the Kohn-Sham equations are a set of eigenequations, and the terms within the brackets in Eq. (1.2.12) can be regarded as Hamiltonian. The bulk of the work involved in a total-energy pseudopotential calculation is the solution of this eigenvalue problem once an approximate expression for the exchange-correlation energy is given.

The simplest method for describing the exchange-correlation energy of an electronic system is to use the local-density approximation (LDA) and this approximation is almost universally used in total-energy pseudopotential calculations [99-100]. In the LDA the exchange-correlation energy of an electronic system is constructed by assuming that the exchange-correlation energy per electron at a point **r** in the electron gas, is equal to the exchange-correlation energy per electron in a homogeneous electron gas that has the same density as the electron gas at point **r**. Thus

$$E_{xc}[n(\boldsymbol{r})] = \int \varepsilon_{XC}(\boldsymbol{r}) n(\boldsymbol{r}) d^3\boldsymbol{r} \tag{1.2.17}$$

$$\frac{\delta E_{xc}[n(\boldsymbol{r})]}{\delta n(\boldsymbol{r})} = \frac{\partial [n(\boldsymbol{r})\varepsilon_{XC}(\boldsymbol{r})]}{\partial n(\boldsymbol{r})} \tag{1.2.18}$$

With

$$\varepsilon_{XC}(\boldsymbol{r}) = \varepsilon_{XC}^{\text{hom}}(\boldsymbol{r})[n(\boldsymbol{r})] \tag{1.2.19}$$

The LDA assumes that the exchange-correlation energy functional is purely local and ignores corrections to the exchange-correlation energy at a point **r** due to nearby inhomogeneities in the electron density.

1.2.3 Exchange and correlation

The wave function of a many-electron system must be antisymmetric under exchange of any two electrons because the electrons are fermions. The antisymmetry of the wave function produces a spatial separation between electrons that have the same spin and thus reduces the Coulomb energy of the electronic system. The reduction in the energy of the electronic system due to the antisymmetry of the wave function is called the exchange energy. It is

straight forward to include exchange in a total energy calculation, and this is generally referred to as the Hartree-Fock approximation.

A more accurate scheme than Thomas-Fermi approximation for treating the kinetic-energy functional of interacting electrons,$T[n]$, is based on decomposing it into one part that represents the kinetic energy of noninteracting particles of density n, i.e., the quantity called above $T_s[n]$, and one that represents the remainder, denoted $T_c[n]$ (the subscripts s and c stand for 'single-particle' and 'correlation', respectively)

$$T[n] = T_c[n] + T_s[n] \tag{1.2.20}$$

$T_s[n]$ is not known exactly as a functional of n but it is easily expressed in terms of the single-particle orbitals $\phi_i(\boldsymbol{r})$ of a noninteracting system with density n, as

$$T_s[n] = -\frac{\hbar^2}{2m}\sum_i^N \int d^3r \phi_i^*(\boldsymbol{r}) \nabla_i{}^2 \phi_i(\boldsymbol{r}) \tag{1.2.21}$$

Because of noninteracting particles, total kinetic energy is a sum of the individual kinetic energies. Since all $\phi_i(\boldsymbol{r})$ are functionals of n, this expression for T_s is an explicit orbital functional but an implicit density functional,$T_s[n] = T_s[\{\phi_i[n]\}]$, where the notation indicates that T_s depends on the full set of occupied orbitalsϕ_i, each of which is a functional of n.

We now rewrite the exact energy functional as

$$E[n] = T[n] + U[n] + V[n] = T_s[\{\phi_i[n]\}] + U_H[n] + E_{xc}[n] + V[n] \tag{1.2.22}$$

Where by definition E_{xc} contains the differences $T - T_s$ (i.e. T_c) and $U - U_H$. This definition shows that a significant part of the correlation energy $E_c$is due to the difference T_c between the noninteracting and the interacting kinetic energies. But still E_{xc} is unknown — although the HK theorem guarantees that it is a density functional. This functional,$E_{xc}[n]$, is called the *exchange-correlation* (*xc*) energy. It is often decomposed as$E_{xc} = E_x + E_c$, where E_x is due

to the Pauli principle (exchange energy) and E_c is due to correlations. (T_c is then a part of E_c.) The exchange energy can be written explicitly in terms of the single-particle orbitals as

$$E_x[\{\phi_i[n]\}] = -\frac{q^2}{2}\sum_{jk}\int d^3r \int d^3r' \frac{\phi_j^*(r)\phi_k^*(r')\phi_j(r')\phi_k(r)}{|r-r'|} \qquad (1.2.23)$$

This is also known as Fock term.

The Coulomb energy of the electronic system can be reduced below its Hartree-Fock value if electrons that have opposite spins are also spatially separated. In this case the Coulomb energy of the electronic system is reduced at the cost of increasing the kinetic energy of the electrons. The difference in the many-body energy of an electronic system and the energy of the system calculated in the Hartree-Fock approximation is called the *correlation energy*. It is however extremely difficult to calculate the correlation energy of complex system. Density-functional theory, try to provide a simple method for describing the effects of exchange and correlation in an electron gas. Hohenberg and Kohn proved that the total energy, including exchange and correlation, of an electron gas (even in the presence of a static external potential) is a unique functional of the electron density.

1.2.4 Pseudopotentials

The fundamental idea of pseudopotential is its application to replace the strong Coulomb potential of the nucleus and the effects of the tightly bound core electrons by an effective ionic potential acting on the valance electrons. Pseudopotential can be generated in an atomic calculation and then used to compute properties of valance electrons in molecules or solids, since the core states remain unchanged.

Pseudopotential theory allows one to replace the strong electron-ion potential with a much weaker potential – a pseudopotential- that describes all the salient features of a valance

electron moving through the solid, including relativistic effects. Thus the original solid is now replaced by pseudo valance electrons and pseudo-ion cores. These pseudopotentials experience exactly the same potential outside the core region as the original electrons but have a much weaker potential inside the core region.

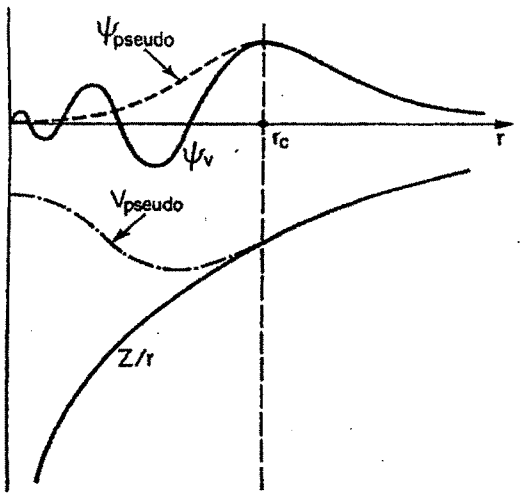

Fig. 1.2.1: Schematic illustration of all-electron (solid lines) and pseudo electron (dashed lines) potentials and their corresponding wave functions. The radius at which all-electron and pseudo electron values match is designated r_c.

1.2.4.1 Need of Pseudopotentials

Use of pseudopotentials make implementation of Plane wave basis set in first principle calculations possible. Although Bloch's theorem states that the electronic wave functions can be expanded using a discrete set of plane waves, a plane-wave basis set is usually very poorly suited to expanding electronic wave functions because, a very large number of plane waves are needed to expand the tightly bound core orbitals and to follow the rapid oscillations of the wave functions of the valance electrons in the core region. An extremely large plane-wave basis set would be required to perform an all-electron calculation, and a vast amount of

computational time would be required to calculate the electronic wave functions. The pseudopotential approximation allows the electronic wave functions to be expanded using a much smaller number of plane-wave basis sets.

It is well known that most physical properties of solids are dependent on the valance electrons to a much greater extent than on the core electrons. The pseudopotential approximation exploits this by removing the core electrons and by replacing them and the strong ionic potential by a weaker pseudopotential that acts on a set of pseudo wave functions rather than the true valance wave functions. An ionic potential, valence wave function and the corresponding pseudopotential and pseudo wave function are illustrated in above Fig. 1.2.1. The valence wavefunctions oscillate rapidly in the region occupied by the core electrons due to strong ionic potential in this region. These oscillations maintain the orthogonality between the core wave functions and the valence wave functions, which is required by the exclusion principle. The pseudopotential is constructed, ideally, so that its scattering properties or phase shifts for the pseudo wave functions are identical to the scattering properties of the ion and the core electrons for the valance wave functions, but in such a way that the pseudo wave functions have no radial nodes in the core region.

The phase shift produced by the ion core is different for each angular momentum component of the valence wave function, and so the scattering from the pseudopotential must be angular momentum dependent. The most general form for a pseudo potential is

$$V_{NL} = \sum_{lm} |lm\rangle V_l \langle lm| \qquad (1.2.24)$$

Where, $|lm>$ are the spherical harmonics and V_l is the pseudopotential for angular momentum l. Acting on the electronic wave function with this operator decomposes the wave function in to spherical harmonics, each of which is then multiplied by the relevant pseudopotential V_l.

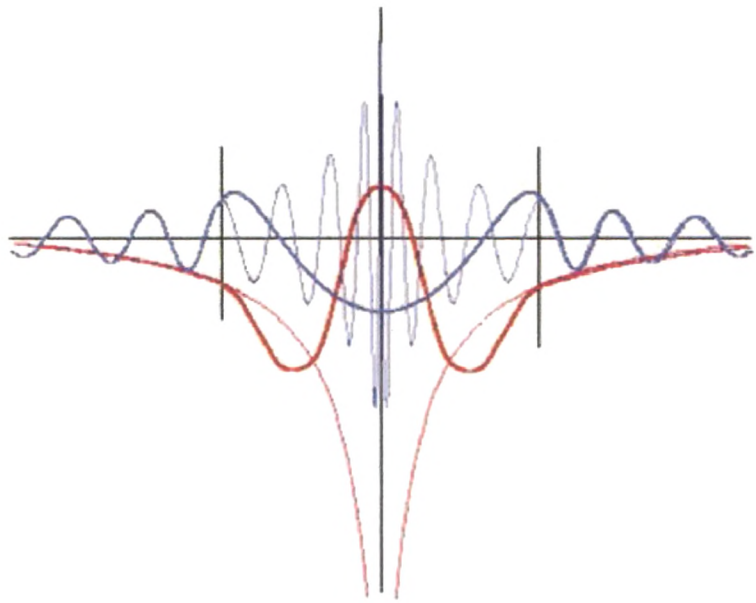

Fig. 1.2.2: A schematic representation of the potentials (red lines) and wave functions (blue lines) for an atom. The real potential and wave function are shown with thin lines, while pseudopotential and wave function are shown in thick lines. Outside the cutoff region/ core region (vertical black lines) the two are identical, and the scattering from the two potentials are indistinguishable.

A pseudopotential that uses the same potential for all the angular momentum components of the wave function is called a local pseudopotential. A local pseudopotential is a function only of distance from the nucleus. While nonlocal pseudopotential uses a different potential for each angular momentum component of the wave function.

A general form of pseudopotential is

$$V_{ps} = V_{ps,\mathrm{loc}} + \sum_l \delta V_l \hat{P}_l \qquad (1.2.25)$$

Where $V_{ps,loc}$ is the local part of the pseudopotential, δV_l is the l^{th} component of the nonlocal part of the pseudopotential, and

$$\hat{P}_l = \sum_{m=-l}^{l} |lm\rangle\langle lm| \qquad (1.2.26)$$

is the projection operator to an angular momentum state *l*. Kleinman and Bylander suggested a form of a fully nonlocal separable pseudopotential[16],

$$V_{ps}^{KB} = V_{ps,loc} + \sum_{lm} \frac{|\phi_{lm}^0 \delta V_l\rangle\langle\delta V_l \phi_{lm}^0|}{\langle\phi_{lm}^0|\delta V_l|\phi_{lm}^0\rangle} \qquad (1.2.27)$$

Whereϕ_{lm}^0)'s are the wave functions of a pseudo atom.

In total energy calculations, the exchange-correlation energy of the electronic system is a function of the electron density. If the exchange-correlation energy is to be desired accurately, it is necessary that outside the core regions the pseudo wave functions and real wave functions be identical, not just in their spatial dependences but also in their absolute magnitudes, so that the two wave functions generate identical charge densities. Adjustment of the pseudopotential to ensure that the integrals of the squared amplitudes of the real and the pseudo wave functions inside the core regions are identical guarantees the equality of the wave functions and pseudo wave functions outside the core region.

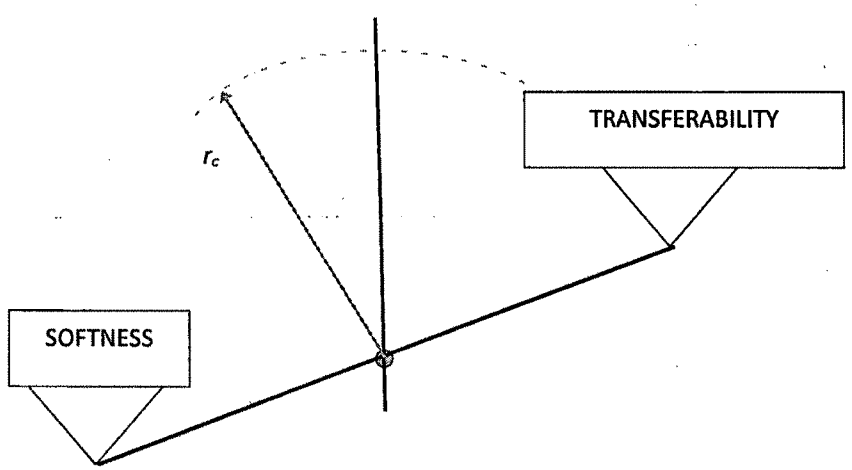

Fig. 1.2.3: Relation between transferability and smoothness depending on r_c for given pseudopotential.

Here, transferability is a measure of the ability of pseudopotential to give accurate description of element in varying environments. And softness depends on the requirement of plane waves to represent the wave functions. Need of a reasonably small set of plane waves suggests softness while need of large number of plane waves suggest that pseudopotential is harder. Many systematic and successful procedures for the development of accurate and transferable pseudopotentials have been developed. Where, proper balance between transferability and softness of pseudopotentials is achieved. [101-107]

1.2.4.2 Norm conserving pseudopotential

As shown in above Fig. 1.2.2 ψ_{pseudo} has no oscillations in core region unlikeψ_v. This pseudo wave function inside the cut off radius must conserve the norm.

$$\int_0^{r_c} |\psi_{pseudo}|^2 r^2 dr = \int_0^{r_c} |\psi_v|^2 r^2 dr \qquad (1.2.28)$$

The most frequently used pseudopotential in first-principles calculations is the norm-conserving pseudopotential technique developed by Hamann *et al.* [102], Bachelet *et al.* [103], as well as the improved version by Troullier and Martins [104]. Where, the added constraint of norm conservation is introduced in order to preserve transferability. The pseudo-wave function obtained using these pseudopotentials have the following characteristics (as shown Fig. 1.2.2).

a. There are no nodes in the pseudo-wave function.

b. The pseudo-wave function agrees with the all-electron wave function outside the inner-shell radius of r_c.

c. The eigenvalue of the valence electron state using pseudopotentials is in accordance with the eigenvalue calculated including the inner shell electrons.

Several groups have proposed modified schemes for generating pseudopotentials aimed at reducing the number of plane waves required to describe properly the electron-ion interaction either focusing on producing improved smoother wavefunctions in the pseudizing process or smoother potentials [105-107]. In all the applications presented here, optimized well-tested norm conserving pseudopotentials have been used. [108]

1.2.5 Supercell approximation

The supercell approximation allows one to deal with aperiodic configurations of atoms within the framework of Bloch's theorem. One simply constructs a large unit cell containing the configuration in question and repeats it periodically throughout space. By studying the properties of the system for larger and larger unit cells, one can gauge the importance of induced periodicity and systematically filter it out.

Concept of Periodic Supercell

Even after application of Kohn-Sham equations there still remains the formidable task of handling an infinite number of noninteracting electrons moving in the static potential of an infinite number of nuclei or ions. Introduction of periodicity and application of Bloch's theorem to the electronic wave functions help to solve two difficulties: (i) calculating wave function for each of the infinite number of electrons in the system and (ii) to expand each wave function extended over the entire solid using finite basis set.

Bloch's theorem states that in a periodic solid each electronic wave function can be written as the product of a cell-periodic part and a wavelike part,

$$\psi_i(\boldsymbol{r}) = \exp[i\mathbf{k}.\boldsymbol{r}]\, f_i(\boldsymbol{r}) \qquad (1.2.29)$$

The cell-periodic part of the wave function can be expanded using a basis set consisting of a discrete set of plane waves whose wave vectors are reciprocal lattice vectors of the crystal,

$$f_i(\boldsymbol{r}) = \sum_{\mathbf{G}} c_{i,G} \exp[i\mathbf{G}.\boldsymbol{r}] \quad (1.2.30)$$

Where the reciprocal lattice vectors **G** are defined by $\mathbf{G}.\boldsymbol{l} = 2\pi m$ for all $\boldsymbol{l}$ where $\boldsymbol{l}$ is a lattice vector of the crystal and m is an integer. Therefore each electronic wave function can be written as a sum of plane waves,

$$\psi_i(\boldsymbol{r}) = \sum_{\mathbf{G}} c_{i,\mathbf{k}+\mathbf{G}} \exp[i(\mathbf{k}+\mathbf{G}).\boldsymbol{r}] \quad (1.2.31)$$

Bloch's theorem states that the electronic wave functions at each **k** point can be expanded in terms of a discrete plane-wave basis set. In principle, an infinite plane-wave basis set is required to expand the electronic wave functions. However, the coefficients $c_{i,\mathbf{k}+\mathbf{G}}$ for the plane waves with small kinetic energy $\left(\hbar^2/2m\right)|\boldsymbol{k}+\boldsymbol{G}|^2$ are typically more important than those with large kinetic energy. Thus the plane wave basis set can be truncated to include only plane waves that have kinetic energies less than some particular cutoff energy. Moreover application of the Bloch theorem allows the electronic wave function to be expanded in terms of a discrete set of plane waves. Thus, introduction of an energy cutoff to the discrete plane-wave basis set produces a finite basis set. The truncation of the plane-wave basis set at a finite cutoff energy leads to an error in the computed total energy. However, it is possible to reduce the magnitude of the error by increasing the value of the cutoff energy until the calculated total energy has converged.

When the plane waves are used as a basis set for the electronic wave functions, the Kohn-Sham equations assume a particularly simple form. Substitution of Eq. (1.2.31) into (1.2.3) and integration over **r** gives,

$$\sum_{\mathbf{G}'}\left\{\left[-\frac{\hbar^2}{2m}\right]|\boldsymbol{k}+\boldsymbol{G}|^2\delta_{\mathbf{G}\mathbf{G}'} + V_{ion}(\mathbf{G}-\mathbf{G}') + V_H(\mathbf{G}-\mathbf{G}') + V_{XC}(\mathbf{G}-\mathbf{G}')\right\}c_{i,\mathbf{k}+\mathbf{G}'} = \varepsilon_i c_{i,\mathbf{k}+\mathbf{G}}$$

(1.2.32)

In this form, the kinetic energy is diagonal, and the various potentials are described in terms of their Fourier transforms. Solution of Eq. (1.2.32) proceeds by diagonalization of a Hamiltonian matrix whose matrix elements $H_{\mathbf{k+G,k+G'}}$ are given by the terms in the brackets above. The size of the matrix is determined by the choice of cutoff energy,

$$\left(\hbar^2/_{2m}\right)|\boldsymbol{k}+\boldsymbol{G}|^2.$$

Nonperiodic systems using idea of supercell

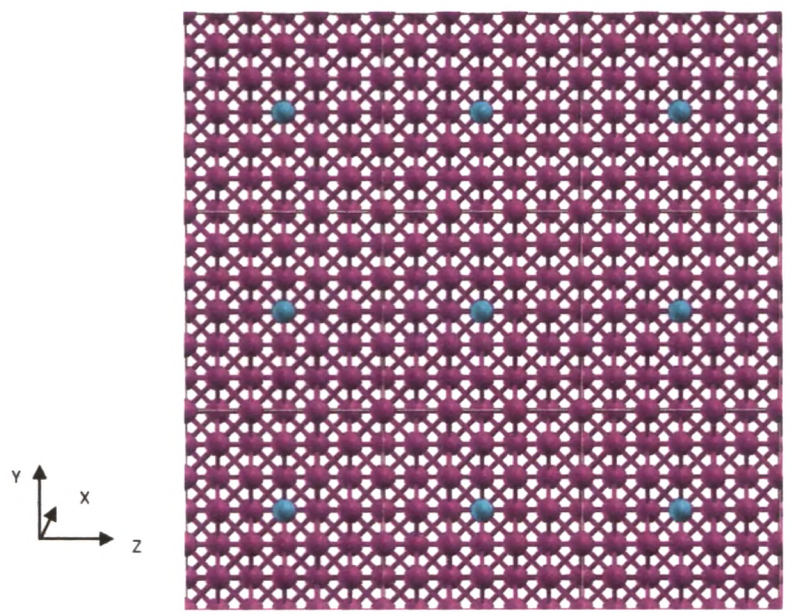

Fig. 1.2.4: Supercell used for Al (pink sphere) bulk crystal with Si point defect (blue sphere)

Calculations using plane-wave basis sets can only be performed on the systems containing defects or crystal surface if a periodic supercell is used. Otherwise a continuous plane-wave basis set would be required which is computationally impractical. The supercell for a point-defect calculation is illustrated in Fig. 1.2.4. The supercell contains the defect surrounded by

across the vacuum region. Moreover the crystal slab must be thick enough so that the two surfaces of each crystal slab do not interact through the bulk crystal.

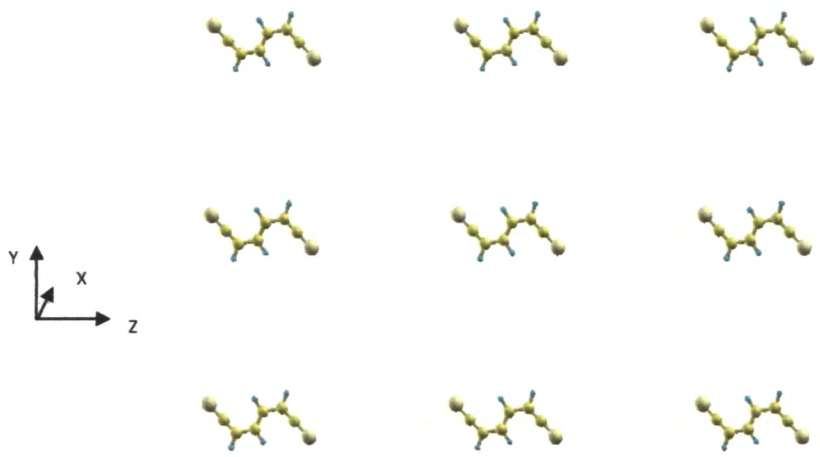

Fig. 1.2.6: Supercell with large vacuum in all three directions, used for SC_6H_4S molecules with S atoms shown by bigger dark yellow spheres, C atoms shown by smaller bright yellow spheres and H shown by blue spheres.

Similarly, for the calculation with molecules one has to keep large enough vacuum in all three directions around the molecule to avoid the interactions between adjacent replicas of molecule. We have studied molecules in this way as illustrated in Fig. 1.2.6.

1.2.6 Algorithm

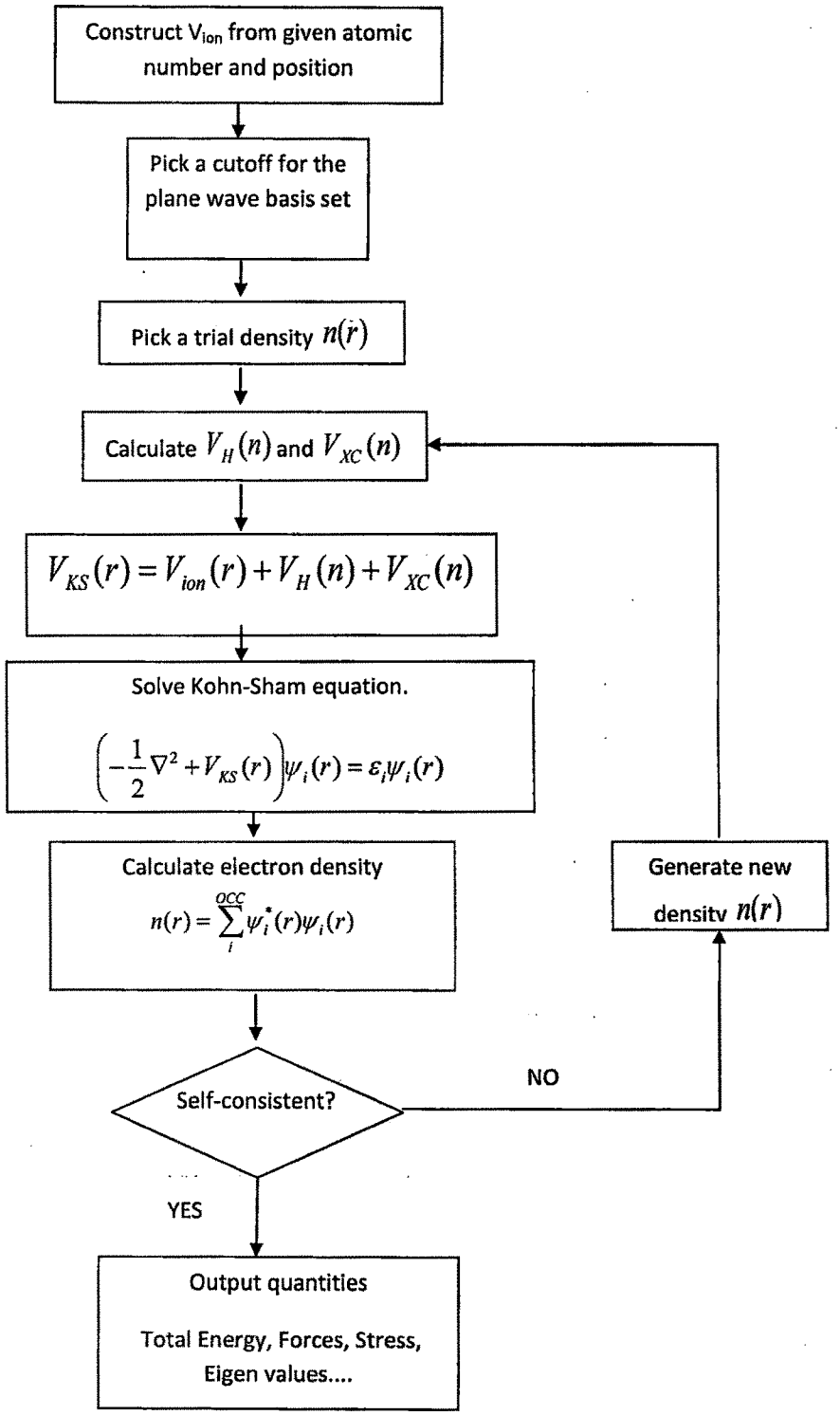

1.3 Electronic Transport Calculations

1.3.1 Electron Transport in bulk

Let us first consider the mechanism of electron conduction in a macroscopic system. In solids, such as metals and semiconductors, electrons in the vicinity of the Fermi level are accelerated by an applied electric field, and undergo inelastic scattering with energy dissipation caused by lattice vibration (phonon) and collisions with impurities. While repeating the process in which electrons are accelerated and inelastically scattered, electrons in general proceed in the direction of the electric field (drift conduction) and reach drift speed, which is proportional to the magnitude of the electric field. As a result, for a conducting wire that is longer than the mean free path of electrons (which is the average distance that electrons proceed without being subjected to scattering; 10 - 50 nm for metallic bulks at room temperature), Ohm's law holds; electric conductance is inversely proportional to the length of the wire and proportional to its cross-sectional area. To bring the essential concepts of the physics behind electron transport, let us consider a simple model that consists of a metallic sample of length L, section A and whose electronic structure is well described by a single electronic band with dispersion relationε_k. Here, because of scattering events with impurities, or with lattice vibrations, electrons may change from one $\vec{k}$ state to another. The scattering rate is quantified by the relaxation timeτ_k, which is the average time an electron in state $\vec{k}$ travels between two scattering events [109]. Suppose first that the sample is in thermodynamic equilibrium so that no net current can be measured. The electrons in the system will fill the states in the band following the Fermi distribution functionf_k. Now if a finite voltage V is supplied by an external source, across the length L of the sample then a static and uniform electric field of modulus $E = -V/L$ is felt in the material. This field causes the electronic population of the material to no longer be in equilibrium. Rather, the

states will be filled according to a new distribution functiong_k. The electric field will also cause a net motion of electrons, so that there will be a finite current density

$$\vec{j} = -2e \int \frac{d\vec{k}}{(2\pi)^3} \overrightarrow{v_k}\, g_k \qquad (1.3.1)$$

Where $\hbar\, \overrightarrow{v_k} = \vec{\nabla}\varepsilon_k$

If the material is isotropic, the current density is parallel to the electric field. If, in addition, E is small enough, the expression for the modulus of the current can be simplified to [109]

$$j = \sigma E = 2e^2 N_F \tau_F^2 E = 2e^2 N_F v_F l E \qquad (1.3.2)$$

Here, $\sigma$is the conductivity of the material, $N_F$is the density of states at Fermi energy, $l = \tau_F v_F$is the average length traversed by an electron between two scattering events. The conductance of the sample

$$G = \frac{A}{L}\sigma = 2e^2 N_F v_F A \frac{l}{L} \qquad (1.3.3)$$

depends on the ratio l/L. for nanostructures, in which nanowires shorter than the mean free path(i.e. the cases where L $\ll$ l) are connected to electrodes, most of electrons proceed without inelastic scattering; instead, they penetrate the nanowires ballistically from one end to the other. This type of conduction is called ballistic transport of electrons. In this case the above expression must be replaced by

$$G = \frac{A}{L}\sigma = 2e^2 N_F v_F A \qquad (1.3.4)$$

In the case of the ballistic transport, the conductance is independent of the length of the nanowires. Furthermore, when the diameter of the cross section of the nanowires becomes as small as the Fermi wavelength of electrons (for example, the Fermi wavelength for gold is 0.52 nm) and thus energy levels are quantized, electrons can pass through the nanowires only via the quantized energy levels. Therefore, a conduction phenomenon that is significantly

different from that having the general macroscopic diffusive-transport characteristics of solids, are observed in ballistic transport.

Conversely, the diffusive regime happens when $L \gg l$ so that each electron that enters the sample on one side will scatter many times before leaving it from the other side. The conductance is in this case small. Notice that the room-temperature mean free path of a metal is of the order of a few nanometres, so that the transport regime of a typical metallic sample is diffusive. In contrast, the room temperature mean free path in a doped semiconductor is much longer, of the order of tens of nanometres. The transport regime of some key components in microelectronic chips is currently crossing over from the diffusive to the ballistic regime.

1.3.2 Electron Transport in Nanoscale systems: The Concept of Conduction Channel

We assume now that the section A is so small that the metallic sample can be regarded as a one-dimensional bar. The criterion to decide if this is so is that the transverse length d is smaller than the Fermi wavelength (for a metal, $\lambda_F \approx 1$ nm; for a doped semiconductor, $\lambda_F \approx 10$–100 nm). If this is the case, then the conductance is related to the conductivity through the equation

$$G = \frac{1}{L}\sigma = 2e^2 N_F v_F \frac{l}{L} \qquad (1.3.5)$$

Which reduces to $G = 2e^2 N_F v_F$ if the sample is ballistic. For a realistic material with a complicated electronic structure, there are M bands that cross the Fermi energy. Further, the one-dimensional density of states at the Fermi energy can be expressed as $N_F = 1/\hbar v_F$ so that the Fermi velocity cancels out and the conductance can be written as

$$G = M\left(2e^2/_h\right) = MG_0 \qquad (1.3.6)$$

where $G_0 = 2e^2/_h$ is defined as the conductance quantum unit and M is the number of bands that cross the Fermi energy . These bands can be viewed as tracks that the electrons can use to move through the sample and are therefore called conduction channels. Imagine finally that the ballistic bar is connected to two identical electrodes that supply the voltage bias V to the bar, and are the source and drain of electrons. There will clearly be a mismatch between the electronic eigenstates of the electrodes and the bar that will be felt by the electrons when they cross the contacts. This mismatch at both sides is a source of scattering for the electrons that cross the contacts, which can be quantified by the transmission probability T_n that an incoming electron will scatter to channel *n* at the bar, or that an outgoing electron at channel *n*, will leave the bar[110-112]. The complete understanding of transport properties requires the knowledge of the transmission coefficients along *each* conducting channel which vary between zero and one. Then the generalized form of the conductance of a system is

$$G = G_0 \sum_n T_n \qquad (1.3.7)$$

1.3.3 The Concept of Junction

The above example of a ballistic bar that bridges two bulk materials is an example of one of the central concepts. A junction is a solid state device which consists of two metallic bulk materials, called electrodes that sandwich something called the extended molecule, as we depict schematically in Fig. 1.3.1. The extended molecule can be anything that permits some electron flow between the electrodes: another material, vacuum, a molecule, a quantum dot,

etc. The small regions in space where the extended molecule and the electrodes attach to each other are called the contacts.

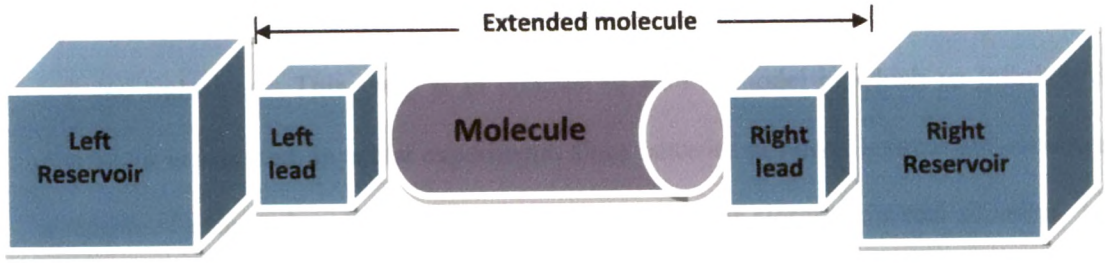

Fig. 1.3.1: Schematic diagram used for electronic transport calculation of nanostructures.

The electrodes are subjected to a voltage bias V, supplied by an external power. It is usually assumed that the whole voltage drop occurs at the region in space that comprises the contacts and the extended molecule, which is therefore called the scattering region. Transport in the extended molecule can be ballistic or diffusive, depending on whether its length is larger or shorter than the mean free path. In the first case, the voltage drop occurs only at the contacts, while in the second, part of this voltage drop also occurs within the extended molecule. Correspondingly, the resistance in the case of ballistic transport is entirely due to the contacts (this is called contact resistance), while in the case of diffusive transport it is due both to the contacts and to scattering events within the extended molecule.

Theories developed by Landauer [110] and Kubo [113] make up the basic theory of electronic transport through metals and semiconductors which is widely used today. The contents of the two theories differ in that; Landauer's theory provides intuitive and simple formulas, while Kubo's theory is a universal theory in which involved mathematical techniques are required. The former is powerful for low-dimensional problems, particularly

We sketch an example in Fig.1.3.2, where the two electrodes are subjected to a very small bias voltage V that shifts their Fermi energy levels by$\pm eV/2$. As shown in the Fig. 1.3.2, the eigenstates at the extended molecule have discrete energy spectra, while the electrodes have continuum of energy states. These two spectra are separated by energy barriers at the contacts. The population of electrons in the electrodes can be described by Fermi distribution functions, whereby all states up to the respective Fermi energy are filled. Because of the Fermi exclusion principle, only those electrons from the left electrode that have energy in the window $(-eV/2, +eV/2)$ can hop into the extended molecule and eventually to the right electrode. There is no way to define Fermi energy at the extended molecule since it is in contact with two electron reservoirs at different chemical potentials. Hence, the extended molecule is a system out of equilibrium whose distribution function is not the Fermi function. In the case of the figure, there is a single state at the extended molecule in the energy window$(-eV/2, +eV/2)$, which is separated from the pristine E_f by the energy E_c. Electrons coming from the left electrode must hop into this state and then move on to the right electrode. Up to now, we have assumed that the energy levels at the extended molecule are discrete, but this is not exactly true: the coupling to the electrodes furnishes them with a finite line width Γ, see Fig. 1.3.3. In other words, the residence time of an electron at the extended molecule can be estimated from$\Delta t\Gamma = h$, where Γ is the probability per unit time that an electron hops into or outside the extended molecule. The transparent regime corresponds to those cases where the energy barriers are low enough that the electrons hop into and out of the extended molecule easily and frequently; the discrete energy levels become wide resonances, whose width Γ is of the order of the width of the electronic bands at the electrodes, W. The tunnelling regime corresponds to the opposite case, where the barriers are quite high, and electrons can only reach the extended molecule via tunnelling events. In this case, the discrete energy levels are sharp resonances, e.g., their line width Γ is approximately

a δ-function. Incoming electrons from one electrode will have a chance to pass to the other only if their energy is finely tuned to the energy of one of the resonances, an effect which is called resonant tunnelling. To summarize, residence times are short in the transparent regime and long in the tunnelling regime. When the residence time in a molecular junction or quantum dot is long, two additional complications may occur. First, electrons may suffer scattering events with an atomic vibration or with another electron, changing its energy. In this case, the phase of the wave function changes and quantum coherence effects are lost or at least blurred. This is the sequential tunnelling regime. In contrast, if inelastic scattering events are absent or rare, the junction is in the coherent tunnelling regime.

1.3.5 The Landauer formalism: equilibrium transport

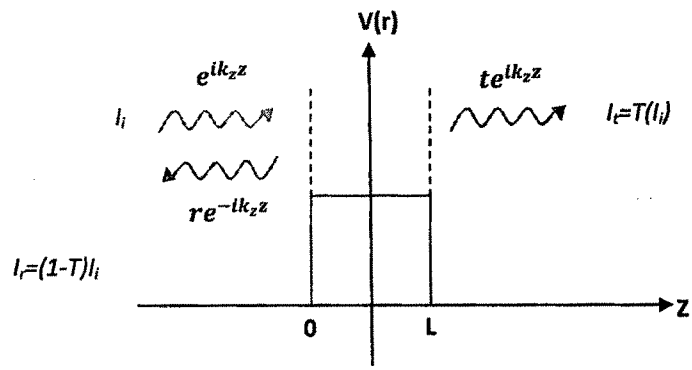

Fig. 1.3.4: Schematic representation of incoming and outgoing wavefunctions scattered by a potential V(r)

The major feature of Landauer's theory is the introduction of electrodes at both ends of a one dimensional conductor for dc conduction, where the conductor is composed of a scatterer and left and right leads. This setup is in contrast to Kubo's model in which an infinitely long

conductor is assumed. In actual experiment, since batteries or power sources are connected to a sample of a finite size via lead wires, Landauer's model is closer to the real situation. Let us consider a scatterer with finite transmission coefficient T. In Landauer approach, the current through a conductor I_t is expressed in terms of the probability that an electron can transmit through it:

$$I_t = T(I_i) \tag{1.3.8}$$

Where, the current of the incident wave I_i can be written as,

$$I_i = \hbar k_z/m \tag{1.3.9}$$

The Landauer-Buttiker formalism [112] associates the conductance of a device with the quantum mechanical transmission probabilities of the one electron wave function as it approaches an arbitrary scattering potential [114]. The problem can be formulated in terms of incoming, $|\Phi_{in}\rangle$ and outgoing, $|\Phi_{out}\rangle$ electron wavefunctions propagating along a one dimensional wire (scattering channel) and scattered by a potential connecting the two leads. Due to the periodic nature of the wire, these wavefunctions have the form of Bloch waves and in absence of a scattering potential, each one contributes with $2e^2/h = G_0$ to the total conductance [112]. We then define the scattering channel as the asymptotic part of the wavefunction deep inside the leads. If the system is multi-dimensional (quasi- 1D, 2D or 3D), several possible Bloch waves with the same energy can propagate through the leads (multi-channel problem). Once the *i*-th channel in the left hand-side reaches the scattering region it can be transmitted to any channel into the right hand-side lead or back scattered into any channels of the left hand-side lead. Fig. 1.3.4 provides a simple example of the transport problem formulated in terms of in-scattering and out-scattering channels: free electrons with energy E are injected from the left and are scattered by a step potential

$$V(z) = \begin{cases} V, & 0 < z < L \\ 0, & elsewhere \end{cases} \quad (1.3.10)$$

As we can see, an incoming electron with wave-vector k_z is partially backscattered with wave-vector $-k_z$ and partially transmitted. The total wavefunction for this problem reads

$$|\Phi_{\text{Total}}\rangle = |\Phi_{in}\rangle + |\Phi_{0L}\rangle + |\Phi_{out}\rangle \quad (1.3.11)$$

With

$$\langle z|\Phi_{\text{Total}}\rangle = \begin{cases} \langle z|\Phi_{\text{in}}\rangle = e^{ik_z z} + re^{-ik_z z}, & z \leq 0 \\ \langle z|\Phi_{0L}\rangle = Ae^{\kappa_z z} + Be^{-\kappa_z z}, & 0 \leq z \leq L \\ \langle z|\Phi_{\text{out}}\rangle = te^{ik_z z}, & z \geq L \end{cases} \quad (1.3.12)$$

Where wave vector k_z is given by$k_z = \frac{\sqrt{2mE}}{\hbar}$, whereas $\kappa_z = \frac{\sqrt{2m(V-E)}}{\hbar}$ can be real (evanescent) or imaginary (propagating) depending on whether $V > E$ or $V < E$ respectively. The coefficients A, B, t and r are determined by solving the scattering equation,

$$-\frac{\hbar^2}{2m}\frac{d^2}{dz^2}\Phi_{Total} + V\Phi_{Total} = E\Phi_{Total} \quad (1.3.13)$$

And imposing the continuity of the total wave function and its derivative at the boundaries of the step potential. Finally

$$|t|^2 + |r|^2 = 1 \quad (1.3.14)$$

i.e., the flux is conserved.

The current through the scatterer $I_t = |t|^2 \frac{\hbar k_z}{m}$ (1.3.15)

Using Eq. (1.3.8) and (1.3.9) in Eq. (1.3.15)

$$T = |t|^2 \quad (1.3.16)$$

1.3.6 PWCOND

We have used PWCOND program [139] contained in quantum Espresso package [140], a method based on plane waves to solve the tip-nanocontact-tip electron scattering problem in real atomic contacts (as depicted in Fig. 1.3.1) and calculate from that the ballistic conductance of open quantum systems via the Landauer-Buttiker formula.. PWCOND follows the methodology derived by Choi and Ihm [141] for *ab initio* treatment of the behavior of electrons in nanostructures (resistive region) between semi-infinite realistic metallic probes. Nonlocality in pseudopotential is included in the calculation for actual solids including realistic metal probes. A major difficulty arises in dealing with the response of the conducting electrons to the nonlocality of the potential, which cannot be determined locally in the multiple scattering processes until the full solution is found. The problem is overcome by use of Kleinman-Bylander–type nonlocal pseudopotential in the Hamiltonian and deriving generalized inhomogeneous differential equations from the self consistent Kohn-Sham equation. Then the equations with the wave-function-matching method for a given electron energy E has been solved.

The course of formulism adopted in the calculation using PWCOND can be summarised as follow:

The efficient and still exact method derived by Choi and Ihm to calculate the transmission matrix of a large system for a given nonlocal potential is applied to the calculation of the conductance based on the Landauer formalism. The self-consistent potential is obtained performing ground state DFT calculations with a Norm-conserving Kleinman-Bylander Pseudopotentials for supercell containing the scattering region (of length L in z direction with$0 \leq z \leq L$) containing some portions of left and right electrodes as leads. A supercell is periodic in xy plane having large vacuum between resistive region and its replicas. A general

form of the Kleinman-Bylander pseudopotentials is discussed in Eqs. (1.2.25-1.2.27). Eq. (1.2.27) can also be written as,

$$V_{ps}^{KB} = V_{ps,loc} + \sum_{lm} Z_l |W_{lm}\rangle\langle W_{lm}| \tag{1.3.17}$$

Where, Z_l is the sign of $\langle \emptyset_{lm}^0 | \delta V_l | \emptyset_{lm}^0 \rangle$ and $W_{lm} = \delta V_l \emptyset_{lm}^0 / \sqrt{|\langle \emptyset_{lm}^0 | \delta V_l | \emptyset_{lm}^0 \rangle|}$.

Now, for this system the self consistent Kohn-Sham equation [112] becomes

$$E\psi(\boldsymbol{r}) = \left[-\frac{\hbar^2}{2m}\right] \nabla^2 \psi(\boldsymbol{r}) + V_{loc}(\boldsymbol{r})\psi(\boldsymbol{r}) + \sum_{\alpha lm} \sum_{\boldsymbol{R}_\perp} Z_l^\alpha W_{lm}^\alpha (\boldsymbol{r} - \boldsymbol{\tau}^\alpha - \boldsymbol{R}_\perp)$$
$$\times \int d^3 \boldsymbol{r}' [W_{lm}^\alpha (\boldsymbol{r} - \boldsymbol{\tau}^\alpha - \boldsymbol{R}_\perp)]^* \psi(\boldsymbol{r}') \tag{1.3.18}$$

Where $\boldsymbol{\tau}^\alpha$ is the position of the αth atom in the supercell, $\boldsymbol{R}_\perp$'s are lattice vectors in the *xy* plane, and $V_{loc}(\boldsymbol{r})$ is the total screened local potential, which is the sum of local ionic pseudopotentials, the electrostatic potential due to valence electrons, and the exchange-correlation potential within the LDA. As in the *xy* plane the system is repeated periodically and in this plane the scattering states propagating at the energy E have the Bloch form and can be classified with a $\boldsymbol{K}_\perp$ index. Different $\boldsymbol{K}_\perp$ do not mix and can be treated separately. Furthermore we consider sufficiently large supercells in the *xy* plane and limit the calculation to the two-dimensional Γ point, $\boldsymbol{K}_\perp = 0$ by applying Bloch theorem we can split Eq. (1.3.18) into a system of equations of ψ and $C_{\alpha lm}$:

$$E\psi(\boldsymbol{r}) = \left[-\frac{\hbar^2}{2m}\right] \nabla^2 \psi(\boldsymbol{r}) + V_{loc}(\boldsymbol{r})\psi(\boldsymbol{r}) + \sum_{\alpha lm} C_{\alpha lm} Z_l^\alpha \sum_{\boldsymbol{R}_\perp} e^{i\boldsymbol{K}_\perp \cdot \boldsymbol{R}_\perp} W_{lm}^\alpha (\boldsymbol{r} - \boldsymbol{\tau}^\alpha - \boldsymbol{R}_\perp) \tag{1.3.19}$$

And

$$C_{\alpha lm} = \int d^3 r' [W_{lm}^{\alpha}(r' - \tau^{\alpha})]^* \psi(r') \quad (1.3.20)$$

The general solution of these inhomogeneous differential equations can be written as:

$$\psi(r) = \sum_n a_n \psi_n(r) + \sum_{\alpha lm} C_{\alpha lm} \psi_{\alpha lm}(r) \quad (1.3.21)$$

Here, a_n's and $C_{\alpha lm}$'s are determined from eq. (1.3.20) and boundary conditions on planes at $z = 0$ an $z = L$. ψ_n are linearly independent solutions of the homogeneous equation derived from eq. (1.3.19) by assumption that all $C_{\alpha lm}$'s are zero. While, $\psi_{\alpha lm}(r)$ is the particular solution for each (α, l, m) of the inhomogeneous equation derived from Eq. (1.3.19) by assuming one of the$C_{\alpha lm}$'s as one and other coefficients zero.

As $\psi_n(r + R_\perp) = \psi_n(r) e^{iK_\perp . R_\perp}$ and there is no periodic boundary conditions imposed along the z direction, we can write,

$$\psi_n(r) = \sum_{G_\perp} \psi_n(G_\perp, z) e^{i(K_\perp + G_\perp).r_\perp} \quad (1.3.22)$$

Where, $G_\perp$'s are the 2D reciprocal lattice vectors in the *xy* plane. The same way, we can represent the local potential as

$$V_{loc}(r) = \sum_{G_\perp} V_{loc}(G_\perp, z) e^{iG_\perp . r_\perp} \quad (1.3.23)$$

And similarly, $\psi_{\alpha lm}(r + R_\perp) = \psi_{\alpha lm}(r) e^{iK_\perp . R_\perp}$ and there is no periodic boundary condition imposed along *z* direction, we can write,

$$\psi_{\alpha lm}(r) = \sum_{G_\perp} \psi_{\alpha lm}(G_\perp, z) e^{i(K_\perp + G_\perp).r_\perp} \quad (1.3.24)$$

Now, for the better numerical accuracy, following scheme is used to calculate$V_{loc}(G_\perp, z)$:

The unit cell is divided in *N* slabs along the *z* direction, where *N* is the number of real-space grid points along the *z* direction used in FFT. Each p^{th} slab of thickness L/N is assigned *z*-independent potential function $V_p(r_\perp)$ such that the analytic Fourier transformation to

momentum space exactly reproduces $V_{loc}(\boldsymbol{G})$ for all$\boldsymbol{G}$'s used in self-consistent calculation, i.e.

$$V_{loc}(\boldsymbol{G}) = \sum_{p=1}^{N} \left[\frac{1}{L}\int_{z_{p-1}}^{z_p} e^{-iG_z z} dz\right] V_p(\boldsymbol{G}_\perp) \tag{1.3.25}$$

Here $z_p = pL/N$ and $\boldsymbol{G}_z = 2\pi q/L$ with condition$\left[-\frac{N}{2}\right] + 1 \leq q \leq [\frac{N}{2}]$.

Thus, when the nonlocal part of the pseudopotentialW_{lm}^{α}, the local potential $V_{loc}(\boldsymbol{G})$ and the energy E are given, we calculate$V_p(\boldsymbol{G}_\perp)$, linearly independent solutions of the homogeneous equation for p^{th} slabψ_n^p and particular solution of the inhomogeneous equation for p^{th} slab$\psi_{\alpha lm}^p$. From the orthonormality amongψ_n^p's and$\psi_{\alpha lm}^p$'s for a given *p*, the recurrence relations between the coefficients of the *pth* and *(p+1)th* slabs are obtained and using these recurrence relations $\psi_n(\boldsymbol{r})$ and $\psi_{\alpha lm}(\boldsymbol{r})$ are found respectively, which gives the $\psi(\boldsymbol{r})$ solutions of eq. (1.3.19) in resistive region($0 \leq z \leq L$).

Similarly inside the electrode unit cell of length d, the general solution of the inhomogeneous eq. (1.3.19) can be obtained and expressed as

$$\psi_k = \sum_n a_{n,k}\psi_n + \sum_{\alpha lm} C_{\alpha lm,k}\psi_{\alpha lm} \tag{1.3.26}$$

Algebraic equations containing$a_{n,k}$'s and$C_{\alpha lm,k}$'s can be arranged into a matrix form

$$AX = e^{ikd}BX \tag{1.3.27}$$

Here, A and B are complex general matrices and X is a column vector containing$a_{n,k}$'s and$C_{\alpha lm,k}$'s. These generalised eigenvalue problem is solved to obtain eigenvaluese^{ikd}'s and corresponding eigenvectorsψ_k's with the LAPACK package. In general, the resulting k is a complex number with real k's showing propagating modes and non-zero imaginary parts giving evanescent modes. These propagating and evanescent modes constitute a complex

band structure of the region [142]. Similarly complex band structure of resistive region is found from previously obtained $\psi_n(\boldsymbol{r})$ and $\psi_{\alpha lm}(\boldsymbol{r})$ for resistive region.

Thus the quantum mechanical current I along the z direction in electrode region for a state ψ is given by,

$$I = \mathrm{Im}\left[\frac{\hbar}{m} d^2\boldsymbol{r}_\perp[\psi(\boldsymbol{r})]^* \frac{\partial}{\partial z}\psi(\boldsymbol{r}) + \frac{2}{\hbar}\sum_{\alpha lm} Z_l^\alpha C_{\alpha lm}^* \int_{\tau_z^\alpha - r_{\alpha l}}^{z} dz' \int d^2\boldsymbol{r}_\perp'[W_{lm}^\alpha(\boldsymbol{r}' - \boldsymbol{\tau}^\alpha)]^* \psi(\boldsymbol{r}')\right] \tag{1.3.28}$$

We now assume that a rightward propagating state ψ_k is incident from the left electrode region and there is no incident wave from right electrode region i.e. the left electrode is assumed to be attached to a source while right electrode is attached to a drain. Now, the wave function ψ of the system can be defined as

$$\psi = \begin{cases} \psi_k + \sum_{k' \in L} r_{kk'}\psi_{k'}, & z \le 0 \\ \sum_n a_n \psi_n + \sum_{\alpha lm} C_{\alpha lm}\psi_{\alpha lm}, & 0 \le z \le L \\ \sum_{k' \in R} t_{kk'}\psi_{k'}, & z \ge L \end{cases} \tag{1.3.29}$$

Here, L and R represent the leftward and rightward propagating states, respectively. Now, this scattering wave function of the whole wire obtained by joining smoothly the solutions in the resistive region with the propagating and the evanescent modes of the electrodes at two interfaces respectively is solved by matching the boundary conditions at the $z = 0$ an $z = L$. At $z = 0$ plane, for atoms α, which are shared by both $z \le 0$ and $0 \le z \le L$ regions, we have

$$C_{\alpha lm} = C_{\alpha lm,k} + \textstyle\sum_{k' \in L} r_{kk'} C_{\alpha lm,k'} \tag{1.3.30}$$

Similarly, at $z = L$ plane, where $z \ge L$ and $0 \le z \le L$ regions shares α atoms,

$$C_{alm} = \sum_{k' \in R} t_{kk'} C_{alm,k'} \quad (1.3.31)$$

With all these boundary conditions, a set of inhomogeneous linear algebraic equations is constructed. The number of equations in the set is the same as that of the undetermined coefficients in ψ. After solving this set of equations we get $t_{kk'}$ for all rightward propagating modesψ_k's. The properly normalised transmission coefficient T_k of the state ψ_k is,

$$T_k = \frac{1}{I_k}(\sum_{k' \in R'} I_{k'} |t_{kk'}|^2) \quad (1.3.32)$$

Here, I_k is the probability current per wire of the state ψ_k given by eq. (1.3.28) and the summation over R' suggest that summation is over the rightward propagating modes not including the evanescent modes so that the matrixT_k is of the dimensions $M_R \times M_L$ where M_R and M_L are the number of propagating modes in right and left electrodes, respectively. The multichannel generalization of the Landauer conductance formula is related to T_k as

$$G = \frac{2e^2}{h} \sum_{k \in R'} T_k \quad (1.3.33)$$

Here, $\frac{2e^2}{h}$ is called the quantum of conductance and denoted byG_0.

1.4 References

1. R. Chau, D. Doyle, M. Doczy, et al., in the Proceedings of the 61st Device Research Conference, 123–126, Salt Lake City, 23–25 June 2003.

2. B. Doris et al., Technical Digest of the IEEE International Device Meeting, 937 (2001).

3. B. Yu et al., Technical Digest of the IEEE International Device Meeting, **267** (2002).

4. A. Nitzan and M. A. Ratner, Science **300,** 1384 (2003).

5. A. Aviram and M. A. Ratner, Chem. Phys. Lett. **52,** 9071 (1974).

6. Latha Venkataraman, Jennifer E. Klare, Colin Nuckolls, Mark S. Hybertsen and Michael L. Steigerwald, Nature **442**, 904 (2006).

7. C. Joachim, J. K. Gimzewski, R. R. Schlittler, and C. Chavy, Phys. Rev. Lett. **74,** 2102 (1995).

8. S. Datta, W. Tian, S. Hong, R. Reifenberger, J. I. Henderson, and C. P. Kubiak, Phys. Rev. Lett. **79**, 2530 (1997).

9. R. H. M. Smit, Y. Noat, C. Untiedt, N. D. Lang, M. C. van Hemert and J. M. van Ruitenbeek, Nature **419**, 906 (2002).

10. M. A. Reed, C. Zhou, C. J. Muller, T. P. Burgin, and J. M. Tour, Science **278**, 252 (1997).

11. C. Jin, H. Lan, L. Peng, K. Suenaga and S. Iijima, Phys. Rev. Lett. **102,** 205501(2009).

12. A. Chuvilin, J. C. Meyer, G. Algara-Siller and U. Kaiser, New Journal of Physics **11,** 083019 (2009).

13. B. Standley, W. Bao, H. Zhang, J. Bruck, C. N. Lau, and M. Bockrath, Nano Lett. **8**, 3345 (2008).

14. T. D. Yuzvinsky, W. Mickelson, S. Aloni, G. E. Begtrup, A. Kis, and A. Zettl, Nano Lett. **6**, 2718 (2006).

15. J. Chen, M. A. Reed, A. M. Rawlett, and J. M. Tour, Science **286**, 1550 (1999).

16. Z. Yao, H. W. C. Postman, L. Balents, and C. Dekker, Nature (London) **402**, 273 (1999).

17. S. J. Tans, A. R. M. Verschueren, and C. Dekker, Nature (London) **393**, 49 (1998).

18. C. Collier, E. Wong, M. Belohradsky, F. Raymo, J. Stoddart, P. Kuekes, R. Williams, and J. Heath, Science **285**, 391 (1999).

19. Y. Huang, X. Duan, Y. Cui, L. Lauhon, K.-H. Kim, and C. Lieber, Science **294**, 1313 (2001).

20. N. Garc´ıa, M. Mu˜noz, and Y. W. Zhao, Phys. Rev. Lett. **82**, 2923 (1999).

21. J. J. Versluijs, M. A. Bari, and J. M. D. Coey, Phys. Rev. Lett. **87**, 26601 (2001).

22. J. Chen and M. A. Reed, Chem. Phys. **281**, 127 (2002).

23. W. Wang, T. Lee, and M. A. Reed, Phys. Rev. B **68**, 035416 (2003).

24. X. Y. Xiao, B. Q. Xu, and N. J. Tao, Nano Lett. **4**, 267 (2004).

25. M. S. Hybertsen, L. Venkataraman, J. E. Klare, A. C. Whalley, M. Steigerwald and C. Nuckolls, J. Phys.: Condens. Matter **20**, 374115 (2008).

26. Y. Teramae, K. Horiguchi, S. Hashimoto, M. Tsutsui, S. Kurokawa, and A. Sakai, Appl. Phys. Lett. **93**, 083121 (2008).

27. S. Datta, Electronic Transport in Mesoscopic Systems (Cambridge University Press, Cambridge, UK, 1995).

28. Tomofumi Tada, Masakazu Kondo, and Kazunari Yoshizawa, J. Chem. Phys. **121**, 8050 (2004).

29. N. D. Lang, Phys. Rev. B **52**, 5335 (1995).

30. M. D. Ventra, S. T. Pantelides, and N. D. Lang, Phys. Rev. Lett. **84**, 979 (2000).

31. A. R. Rocha and S. Sanvito, Phys. Rev. B **70**, 94406 (2004).

32. C. Zhang, X.-G. Zhang, P. S. Krstic, Hai-ping Cheng, W. H. Butler and J. M. MacLaren, PHYSICAL REVIEW B **69**, 134406 (2004).

33. F. Evers, F. Weigend, and M. Koentopp, Phys. Rev. B **69**, 235411 (2004).

34. H. J. Choi and J. Ihm, Phys. Rev. B **59**, 2267 (1999).

35. L. Kong, J. R. Chelikowsky, J. B. Neaton and S. G. Louie, Phys. Rev. B **76**, 235422 (2007).

36.]. Burke K, Car R and Gebauer R, *Phys. Rev. Lett.* **94**, 146803(2005).

37. C. Beenakker, Phys. Rev. B **44**, 1646 (1991).

38. R. Gebauer and R. Car, Phys. Rev. B **70**, 125324 (2004).

39. G. Stefanucci and C-O Almbladh, Phys. Rev. B **69**, 195318 (2004).

40. M. D. Ventra and T. N. Todorov, J. Phys.: Condens. Matter **16**, 8025(2004).

41. S. H. Ke, H. U. Baranger, W. Yang, J. Chem. Phys. **123**, 114701 (2005).

42. K.H. Müller, Phys. Rev. B **73**, 045403 (2006).

43. Z. Qian, S. Hou, J. Ning, R. Li, Z. Shen, X. Zhao and Z. Xue, J. Chem. Phy. **126**, 084705 (2007).

44. X. Feng, O. Bengone, M. Alouani, S. Lebègue, I. Rungger and S. Sanvito, Phys. Rev. B **79**, 174414 (2009).

45. J. M. C. Rauba, M. Strange, and K. S. Thygesen, Phys. Rev. B **78**, 165116 (2008).

46. V. M. García-Suárez and C. J. Lambert, Phys. Rev. B **78**, 235412 (2008).

47. R. Stadler and K. W. Jacobsen, Phys. Rev. B **74**, 161405R (2006).

48. Z. Zhang, Z. Yang, J. Yuan and M. Qiu, J. Chem. Phy. **128**, 044711 (2008).

49. M. M. Fadlallah, C. Schuster, U. Schwingenschlogl, T. Wunderlich and S Sanvito, J. Phys.: Condens. Matter **21**, 315001 (2009).

50. Y. Xue and M. A. Ratner, Phys. Rev. B **68**, 115407 (2003).

51. F. Pauly, J. K. Viljas, J. C. Cuevas and G. Schon, Phys. Rev. B **77**, 155312 (2008).

52. D. J. Mowbray, G. Jones and K. S. Thygesen, J. Chem. Phy. **128**, 111103 (2008).

53. Z. H. Zhang, Z. Yang, J. H. Yuan, H. Zhang, X. Q. Ding and M. Qiu, J. Chem. Phy. **129**, 094702 (2008).

54. C. M. Finch, S. Sirichantaropass, S. W. Bailey, I. M. Grace, V. M. Garcia-Suarez and C. J. Lambert, J. Phys.: Condens. Matter **20**, 022203 (2008).

55. S. Martin, D. Z. Manrique, V. M. Garcia-Suarez, W. Haiss, S. J. Higgins, C. J. Lambert and R. J. Nichols, Nanotechnology **20**, 125203(2009).

56. C. B. George, M. A. Ratner and J. B. Lambert, J. Phys. Chem. A **113**, 3876 (2009).

57. Y. X. Zhou, F. Jiang, H. Chen, R. Note, H. Mizuseki and Y. Kawazoe, J. Chem. Phy. **128**, 044704 (2008).

58. Ž. Crljen, A. Grigoriev and G. Wendin, K. Stokbro, Phys. Rev. B **71**, 165316 (2005).

59. Y. X. Zhou, F. Jiang, H. Chen, R. Note, H. Mizuseki and Y. Kawazoe, Phys. Rev. B **75**, 245407 (2007).

60. F. Pauly, J. K. Viljas and J. C. Cuevas, Phys. Rev. B **78**, 035315 (2008).

61. N. D. Lang, Phys. Rev. Lett. **97**, 1357 (1997).

62. S Tongay, S Dag, E Durgun, R T Senger and S Ciraci, J. Phys.: Condens. Matter **17**, 3823–3836 (2005);

63. Hosein Cheraghchi and Keivan Esfarjani: Phys. Rev. **B 78**, 085123 (2008);

64. S. K. Ambavale and A. C. Sharma: J. Comput. Theor. Nanosci. 6, 1549-1555 (2009).

65. Christopher Roland, Vincent Meunier, Brian Larade, and Hong Guo: Phys. Rev. **B 66**, 035332 (2002);

66. Z.X. Dai, X.Q. Shi, XX.H. Zheng, X.L. Wang and Z. Zeng: Phys. Rev. **B 75**, 155402 (2007).

67. Lingzhu Kong, James R. Chelikowsky: Phys. Rev. **B 77**, 073401 (2008).

68. G. Q. Li, J. Cai, J. K. Denng, A. R. Rocha, S. Sanvito: App. Phys. Lett. **92**, 163104 (2008);

69. Thushari Jayasekera and JWMintmire: Nanotechnology **18** (2007) 424033.

70. A. N. Andriotis, Ernst Richter, Madhu Menon: App. Phys. Lett. **91**, 152105 (2007);

71. Lian Sun, Yafei Li, Zhenyu Li, Qunxiang Li, Zhen Zhou, Zhongfang Chen, Jinlong Yang, J. G. Hou, J. Chem. Phys. **129**, 174114 (2008);

72. Masayuki Yamamoto, Yositake Takane, and Katsunori Wakabayashi, Phys. Rev. **B 79**, 125421 (2009).

73. Dragan Stojkovic, Peihong Zhang, and Vincent H. Crespi: Phys. Rev. Lett. **87**, 125502 (2001);

74. Jia-Lin Zhu, Fu-Fang Xu and Yu-Feng Jia: Phys. Rev. **B 74**, 155430 (2006).

75. Ye-Fei Li, Bing-Rui Li, and Hao-Li Zhang J. Phys.: Condens. Matter **20**, 415207 (2008).

76. W. D. Wheeler1, and Yu. Dahnovsky: J. Chem. Phys. **129**, 154112 (2008).

77. C. Morari, G.-M. Rignanese and S. Melinte: Phys. Rev. **B 76**, 115428 (2007).

78. Ž. Crljen, A. Grigoriev and G. Wendin, K. Stokbro: Phys. Rev. **B 71**, 165316 (2005).

79. D. J. Mowbray, G. Jones, and K. S. Thygesen: J. Chem. Phys.**128**, 111103 (2008).

80. Z. Crljen and G. Baranovic: Phys. Rev. Lett. **98**, 116801 (2007);

81. Jeremy S. Evans, Chiao-Lun Cheng, and Troy Van Voorhis: Phys. Rev. B **78**, 165108 (2008).

82. Hugh Dalgleish, George Kirczenow: Phys. Rev. B **73**, 235436 (2006);

83. V. B. Engelkes, J. M. Beebe, and C. D. Frisbie: J. Am. Chem. Soc. **126**, 14287 (2004).

84. Ronaldo J. C. Batista, Pablo Ordejón, Helio Chacham, and Emilio Artacho; Phys. Rev. **B 75**, 041402(R) (2007).

85. Y. X. Zhou, F. Jiang, and H. Chen, R. Note, H. Mizuseki, and Y. Kawazoe: J. Chem. Phys. **128**, 044704 (2008).

86. W. Kohn, Rev. Mod. Phys. **71**, 1253 (1999).

87. J. A. Pople, Rev. Mod. Phys. **71**, 1267 (1999).

88. P. Hohenberg and W. Kohn Phys. Rev. **136**, B864 (1964).

89. W. Kohn and L. J. Sham Phys. Rev. **140**, A1133 (1965).

90. Density Functional Theory of Atoms and Molecules, R.G. Parr and W. Yang (Oxford press, New York, 1989).

91. The ABC of DFT, Kieron Burke, http://chem.ps.uci.edu/~kieron/dft/book/ (2007).

92. Introduction to Nanoscience and Nanotechnology: A Workbook, M. Kuno.

93. Ab initio Molecular Dynamics for Metallic Systems (thesis), Nicola Marzari (1996).

94. M.C. Payne, M. P. Teter, D.C. Allan, T.A. Arias, J.D. Joannopoulos ; Rev. Mod. Phy. **64**, 1045 (1992).

95. First-Principles Calculations in Real-Space Formalism, Electronic Configurations and Transport Properties of Nanostructures; Kikuji Hirose, Tomoya Ono, Yoshitaka Fujimoto, Shigeru Tsukamoto, Imperial College Press (2005).

96. Theoretical and computational aspects of electronic transport at the nanoscale (thesis) Alexandre Reily Rocha; (2007).

97. Measurement of Single-Molecule Conductance; Fang Chen, Joshua Hihath, Zhifeng Huang, Xiulan Li, and N.J. Tao; Annu. Rev. Phys. Chem., **58**, 535–64 (2007).

98. A Bird's-Eye View of Density-Functional Theory, Klaus Capelle; arXiv:cond-mat/0211443v5 [cond-mat.mtrl-sci] (2006).

99. D. M. Ceperley and B. J. Alder, Phys. Rev. Lett. **45,** 566 (1980).

100. J. P. Perdew, J. A. Chevary, S. H. Vosko, K. A. Jackson, M. R. Peder son, D. J. Singh and C. Fiolhais, Phys. Rev. B **46**, 6671 (1992).

101. L. Kleinman and D. M. Bylander, Phys. Rev. Lett. **48**, 1425 (1982).

102. D. R. Hamann, M. Schluter and C. Chiang, Phys. Rev. Lett. **43**, 1494 (1979).

103. Bachelet G.B., Hamann D.R. and Schliiter M., Phys. Rev. B **26**, 8, 4199 (1982).

104. N. Troullier and J.L. Martins, Phys. Rev. B **43**, 1993 (1991).

105. A. M. Rappe, K. M. Rabe, E. Kaxiras and J. D. Joannopoulos, Phys. Rev. **B. 41**, 1227 (1990).

106. J. S. Lin, A. Qteish, M. C. Payne and V. Heine, Phys. Rev. **B** 47, 4174 (1993).

107. D. Vanderbilt, Phys. Rev. B. **41**, 7892 (1990).

108. We used pseudopotentials C.pz-vbc.UPF for C; Al.vbc.UPF for Al; S.pz-bhs.UPF for S, H.vbc.UPF for H and Si.vbc.UPF from the http://www.quantum-espresso.org distribution.

109. Solid State Physics, N. W. Ashcroft and N. D. Mermin, Thomson Asia Pte. Ltd, Singapore (2005).

110. R. Landauer; IBM J. Res. Dev. **1**, pp. 223-231, (1957).

111. M. Buttiker, Phys. Rev. Lett. **57**, 1761 (1986).

112. M. Buttiker, Y. Imry, R. Landauer and S. Pinhas, Phys. Rev. B **31**, 6207 (1985).

113. R. Kubo; J. Phys. Soc. Jpn. **12**, 6, 570 (1957).

114. S. Datta, Electronic Transport in Mesoscopic Systems, Cambridge University Press (1995).

115. Quantum Transport: Atom to Transistor, Supriyo Datta; New York, Cambridge University Press (2005).

116. Electrical Transport in Nanoscale Systems, M. D. Ventra; Cambridge University Press (2008).

117. Electronic structure Basic Theory and Practical Methods, Richard M. Martin; Cambridge University Press (2004).

118. Density functional calculations of nanoscale conductance, Max Koentopp, Connie Chang, Kieron Burke and Roberto Car; J. Phys.: Condens. Matter 20, 083203 (2008).

119. From microelectronics to molecular spintronics: an explorer's travelling guide, Jaime Ferrer and Vı´ctor M. Garcı´a-Su_arez; J. Mater. Chem., 19, 1696 (2009).

120. Transport in Nanostructures, David K. Ferry, Stephen M. Goodnick, Jonathan Bird; Cambridge University Press (2009).

121. S. Sanvito and C. J. Lambert, J. H. Jefferson, A. M. Bratkovsky, Phys. Rev. B **59**, 11936 (1999).

122. J. Taylor, H. Guo and J. Wang, Phys. Rev. B, **63**, 245407 (2001).

123. M. Brandbyge, J. L. Mozos, P. Ordejon, J. Taylor, and K. Stokbro, Phys. Rev. B, **65**, 165401(2002).

124. F. Evers, F. Weigend, and M. Koentopp, Phys. Rev. B **69**, 235411 (2004).

125. N. Sai, M. Zwolak, G. Vignale and M. D. Ventra, Phys. Rev. Lett. **94**, 186810 (2005).

126. S. V. Faleev, F. Léonard, D. A. Stewart and M. Schilfgaarde, Phys. Rev. B **71**, 195422 (2005).

127. M. Koentopp and K. Burke, F. Evers, PHYSICAL REVIEW B **73**, 121403R (2006).

128. T. Shimazaki, Y. Xue, M. A. Ratner, K. Yamashita, J. Chem. Phys. **124**, 114708 (2006).

129. X. Qian, J. Li, X. Lin, and S. Yip, Phys. Rev. B **73**, 035408 (2006).

130. A. D. Corso, A. Smogunov and E. Tosatti, Phys. Rev. B **74**, 045429 (2006).

131. C. Cheng, J. S. Evans and T. V. Voorhis, Phys. Rev. B **74**, 155112 (2006).

132. C. Toher and S. Sanvito, Phys. Rev. Lett. **99**, 056801 (2007).

133. J. R. Reimers, G. C. Solomon, A. Gagliardi, A. Bilic, N. S. Hush, T. Frauenheim, A. D. Carlo and A. Pecchia, J. Phys. Chem. A **111**, 5692 (2007).

134. H. J. Choi, M. L. Cohen and S. G. Louie, Phys. Rev. B **76**, 155420 (2007).

135. T. Frederiksen, M. Paulsson, M. Brandbyge and A. P. Jauho, Phys. Rev. B **75**, 205413 (2007).

136. A. Bagrets, N. Papanikolaou and I. Mertig, Phys. Rev. B **75**, 235448 (2007).

137. T. Ozaki, K. Nishio and H. Kino, Phys. Rev. B **81**, 035116 (2010).

138. N. D. Lang, Phys. Rev. B **36**, 8173 (1987).

139. Alexander Smogunov, Andrea Dal Corso and Erio Tosatti, Phys. Rev. B **70**, 045417 (2004).

140. Paolo Giannozzi et al, J. Phys. Condens. Matter **21** (2009) 395502; http://www.quantum-espresso.org.

141. H. J. Choi and J. Ihm, Phys. Rev. B 59, 2267 (1999).

142. D. L. Smith and C. Mailhiot, Rev. Mod. Phys. **62**, 173 (1990).